

Different resistivity response to spin density wave and superconductivity at 20 K in $\text{Ca}_{1-x}\text{Na}_x\text{Fe}_2\text{As}_2$

G. W. U., H. Chen, T. W. U., Y. L. Xie, Y. J. Yan, R. H. Liu, X. F. Wang, J. J. Ying, and X. H. Chen
Hefei National Laboratory for Physical Science at Microscale and Department of Physics,
University of Science and Technology of China,
Hefei, Anhui 230026, P. R. China

(Dated: February 20, 2024)

We report that intrinsic transport and magnetic properties, and their anisotropy from high quality single crystal CaFe_2As_2 . The resistivity anisotropy (ρ_c/ρ_{ab}) is ~ 50 , and less than 150 of BaFe_2As_2 , which arises from the strong coupling along c -axis due to an apparent contraction of about 0.13 nm compared to BaFe_2As_2 . Temperature independent anisotropy indicates that the transport in ab plane and along c -axis direction shares the same scattering mechanism. In sharp contrast to the case of parent compounds $\text{RFeAsO}_{1-x}\text{F}_x$ (R = rare earth) and MFe_2As_2 (M = Ba and Sr), spin-density-wave (SDW) ordering (or structural transition) leads to a steep increase of resistivity in CaFe_2As_2 . Such different resistivity response to SDW ordering is helpful to understand the role played by SDW ordering in Fe-based high- T_c superconductors. The susceptibility behavior is very similar to that observed in single crystal BaFe_2As_2 . A linear temperature dependent susceptibility occurs above SDW transition of about 165 K. Partial substitution of Na for Ca suppresses the SDW ordering (anomaly in resistivity) and induces occurrence of superconductivity at ~ 20 K.

PACS numbers: 71.27.+a; 71.30.+h; 72.90.+y

The discovery of superconductivity at 26 K in $\text{LaO}_{1-x}\text{F}_x\text{FeAs}$ ($x=0.05-0.12$) [1], and T_c surpassing 40 K beyond Mott limit of 39 K predicted by BCS theory in $\text{RFeAsO}_{1-x}\text{F}_x$ by replacing La with other trivalent R with smaller ionic radii [2, 3, 18] have generated much interest for extensive study on such iron-based superconductors, which is second family of high- T_c superconductors except for the high- T_c cuprates. Such Fe-based superconductor shares some similarity with cuprates. They adopt a layered structure with Fe layers sandwiched by two As layers, each Fe is coordinated by As tetrahedron. Similar to the cuprates, the Fe-As layer is thought to be responsible for superconductivity, and R-O layer is carrier reservoir layer to provide electron carrier. The electron carrier induced transfers to Fe-As layer to realize superconductivity. Electronic properties are dominated by the Fe-As triple-layers, which mostly contribute to the electronic state around Fermi level.

Recently, the ternary iron arsenide BaFe_2As_2 shows superconductivity at 38 K by hole doping with partial substitution of potassium for barium [5]. This material is ThCr_2Si_2 -type structure. There exists single FeAs layer in unit cell in RFeAsO system, while there are two FeAs layers in an unit cell in BaFe_2As_2 . These parent compounds share common features: an anomaly appears in resistivity and such anomaly is associated with a structure transition and spin density wave (SDW) ordering. The parent material LaOFeAs shows an anomaly in resistivity at 150 K which is associated with the structural transition at ~ 150 K and a SDW transition is observed at ~ 134 K [1, 6]. An anomaly in resistivity occurs at ~ 140 K in BaFe_2As_2 and susceptibility shows an antiferromagnetic SDW ordering at almost

the same temperature [7]. Neutron scattering further indicates that the antiferromagnetic SDW ordering and structural transition happen at the same temperature coinciding with the anomaly in resistivity [8]. In all systems of RFeAsO (R = rare earth) and BaFe_2As_2 and SrFe_2As_2 , SDW ordering (or structural transition) leads to a steep decrease of resistivity [1, 7, 9, 10, 11, 12]. Such structure and SDW instabilities are suppressed, and superconducting is induced and the anomaly in resistivity is completely suppressed by electron- and hole-doping in $\text{RFeAsO}_{1-x}\text{F}_x$ system [1, 9, 10] and $\text{M}_{1-x}\text{K}_x\text{Fe}_2\text{As}_2$ (M = Ba, Sr) [5, 11, 12]. Here we reported the anisotropy in resistivity and susceptibility in single crystal CaFe_2As_2 . The resistivity anisotropy is ~ 50 , and less than 150 of BaFe_2As_2 [7], this is consistent with an apparent contraction in c -axis lattice relative to BaFe_2As_2 . It is striking that the resistivity increases when SDW ordering occurs in CaFe_2As_2 , in sharp contrast to that SDW ordering leads to steep decrease in resistivity in all other parent compounds RFeAsO and MFe_2As_2 (M = Ba and Sr). Substitution of Na for Ca leads to suppression of the SDW ordering and structural transition, and induces superconductivity at ~ 20 K. Such resistivity response to SDW ordering will be helpful to understand the role played by SDW ordering in Fe-based high- T_c superconductors.

High quality single crystals of CaFe_2As_2 were grown by self-flux method, which is similar to that described in our earlier paper about growth of BaFe_2As_2 single crystals with FeAs as flux [7]. Many shining plate-like CaFe_2As_2 crystals were obtained. The typical dimensional is about $1 \times 1 \times 0.05 \text{ mm}^3$. Polycrystalline samples of $\text{Ca}_{1-x}\text{Na}_x\text{Fe}_2\text{As}_2$ was synthesized by solid state

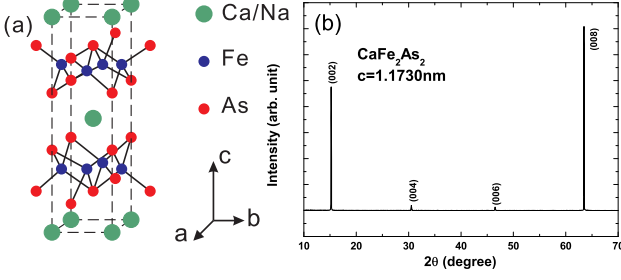


FIG. 1: (a): Crystal structure of CaFe_2As_2 ; (b): Single crystal x-ray diffraction pattern of CaFe_2As_2 , only (00l) diffraction peaks show up, suggesting that the c-axis is perpendicular to the plane of the plate.

reaction method using CaAs , NaAs and Fe_2As as starting materials. CaAs was presynthesized by heating Ca lumps and As powder in an evacuated quartz tube at 923 K for 4 hours. NaAs was prepared by reacting Na lumps and As powder at 573 K for 4 hours, Fe_2As was obtained by reacting the mixture of element powders at 973 K for 4 hours. The raw materials were accurately weighed according to the stoichiometric ratio of $\text{Ca}_{1-x}\text{Na}_x\text{Fe}_2\text{As}_2$, then the weighed powders were thoroughly grounded and pressed into pellets. The pellets were wrapped with Ta foil and sealed in evacuate quartz tubes. The sealed tubes were heated to 1203 K and annealed for 15 hours. The sample preparation process except for annealing was carried out in glove box in which high pure argon atmosphere is filled.

The crystal structure of $\text{Ca}_{1-x}\text{Na}_x\text{Fe}_2\text{As}_2$ is shown in Fig.1 (a), which is the same as BaFe_2As_2 with the tetragonal ThCr_2Si_2 -type compound [14]. The layers of edge-sharing Fe_4S_4 -tetrahedra are separated by Ca atom layers. Fig.1 (b) shows the single crystal x-ray diffraction pattern of CaFe_2As_2 . Only (00l) diffraction peaks are observed, it suggests that the crystallographic c-axis is perpendicular to the plane of the plate-like single crystal. Table 1 shows the crystallographic data of single crystal CaFe_2As_2 at room temperature. X-ray diffraction intensity data measurement was performed at 297 K (Mo K radiation, $\lambda = 0.71073 \text{ \AA}$) using a Gemini Super (Oxford diffraction). All the structures were solved by Patterson methods and refined by full-matrix least-squares methods with SHELX-97 [15]. For comparison, the data of BaFe_2As_2 reported by Rotter et al [13] are also listed in Table 1. Both the CaFe_2As_2 and BaFe_2As_2 have the same space group. The lattice parameters of CaFe_2As_2 is much smaller than that of BaFe_2As_2 . Compared the average bond lengths of CaFe_2As_2 with BaFe_2As_2 , it is found that the length of Ca-As bond is much smaller than Ba-As bond. It indicates that the interaction between the Ca layer and FeAs layer is much stronger than

TABLE I: Crystallographic data of CaFe_2As_2 . For comparison, the data of BaFe_2As_2 are also listed, the data are from Ref.13.

Temperature= 297K	CaFe_2As_2	BaFe_2As_2
Space group	I4/mmm	I4/mmm
a (nm)	0.3872 (9)	0.39625 (1)
b (nm)	0.3872 (9)	0.39625 (1)
c (nm)	1.1730 (2)	1.30168 (3)
V (nm ³)	0.17594 (5)	0.20438 (1)
Atomic parameters:		
Ca (Ba)	2a (0, 0, 0)	2a (0, 0, 0)
Fe	4d ($\frac{1}{2}, 0, \frac{1}{4}$)	4d ($\frac{1}{2}, 0, \frac{1}{4}$)
As	4e (0, 0, z)	4e (0, 0, z)
	z= 0.3665 (9)	z= 0.3545 (1)
Average Bond lengths (nm):		
Ca (Ba) As	0.3154 (0)	0.3379 (6)
Fe As	0.2370 (9)	0.2397 (6)
Fe Fe	0.2738 (7)	0.2799 (6)
Average Bond angles (deg):		
As Fe As ₁	109.5 (2)	111.3 (6)
As Fe As ₂	109.4 (6)	108.5 (6)

that between the Ba layer and FeAs layer.

Temperature dependence of susceptibility measured under magnetic field of $H = 5 \text{ T}$ applied within ab-plane and along c-axis is shown in Fig.2, respectively. It should be pointed out that an anisotropy between $H \parallel ab$ plane and along c-axis is observed, but these data are not corrected by demagnetization factor. Susceptibility decreases monotonically for the magnetic field applied within ab-plane and along c-axis, and shows a linear temperature dependence above a characteristic temper-

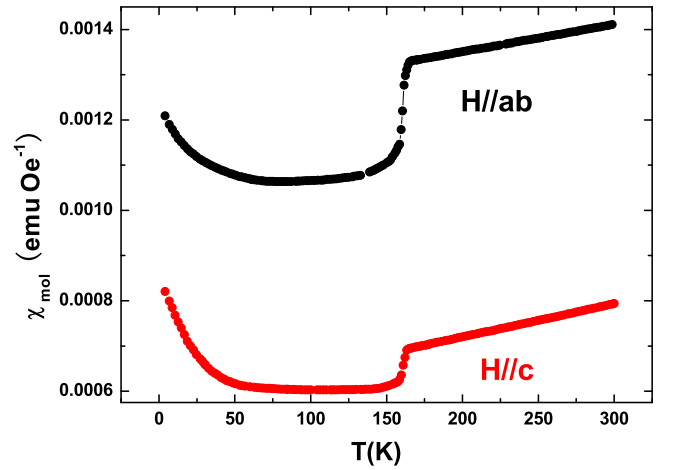


FIG. 2: Temperature dependence of susceptibility measured under $H = 5 \text{ Tesla}$ applied within ab-plane and along c-axis, respectively, for single crystal CaFe_2As_2 .

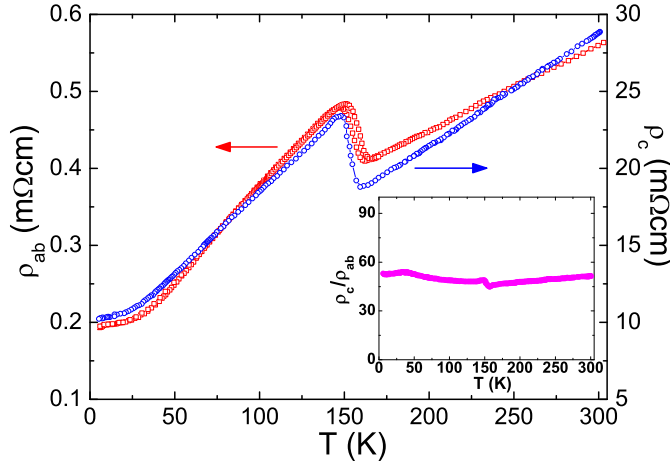


FIG. 3: Temperature dependence of in-plane and out-of-plane resistivity ($\rho_{ab}(T)$ (squares) and $\rho_c(T)$ (circles)) for single crystal CaFe_2As_2 . A hysteresis in $\rho_{ab}(T)$ is observed with cooling and heating measurements. Inset shows temperature dependence of the anisotropy of resistivity (ρ_c/ρ_{ab}). The anisotropy ρ_c/ρ_{ab} is independent of temperature, indicating that the transport in ab plane and along c -axis direction shares the same scattering mechanism.

ature of 165 K. At 165 K, the susceptibility shows a rapid decrease which is ascribed to occurrence of antiferromagnetic spin-density wave. Below 165 K, susceptibility decreases more strongly than T -linear dependence. In low temperatures, a Curie-Weiss-like behavior in susceptibility is observed. These behaviors are very similar to the susceptibility behavior reported in single crystal BaFe_2As_2 [7]. The magnitude of susceptibility is almost the same as that of BaFe_2As_2 . The susceptibility behavior observed in both BaFe_2As_2 and CaFe_2As_2 is very similar to that of antiferromagnetic SDW pure Cr [16], in which a temperature linear dependence persists to the occurrence temperature of SDW.

Figure 3 shows temperature dependence of in-plane and out-of-plane resistivity. Both in-plane and out-of-plane resistivity show similar temperature dependent behavior. In-plane and out-of-plane resistivities show almost a linear temperature dependence above 165 K, and a steep increase at 165 K, then changes to metallic behavior. As shown in Fig. 3, a hysteresis around 165 K is observed with cooling and heating measurements, suggesting a possible first-order transition at 165 K. This transition temperature coincides with the SDW transition observed in susceptibility as shown in Fig. 2. It indicates that the SDW ordering leads to a steep increase in resistivity. Such resistivity response to the SDW transition is in sharp contrast to that for all other parent compounds RFeAs ($\text{R} = \text{rare earth}$) and BaFe_2As_2 and SrFe_2As_2 [1, 7, 9, 10, 11, 12], in which SDW ordering (or structural transition) leads to a steep decrease

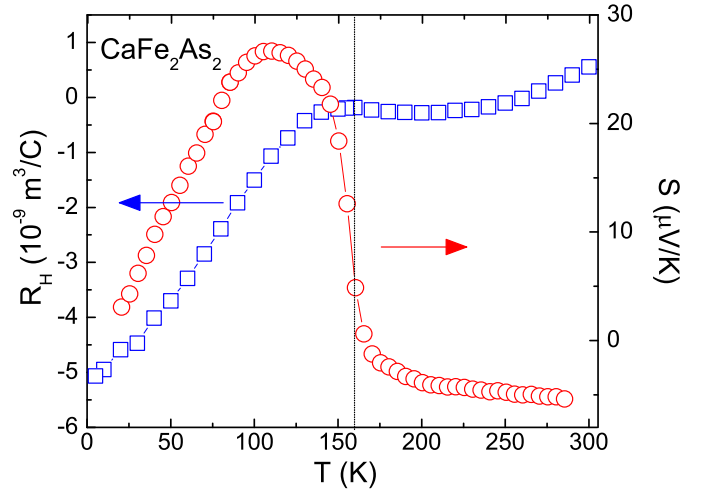


FIG. 4: The temperature dependence of Hall coefficient and thermoelectric power (TEP) of single crystal CaFe_2As_2 .

of resistivity. Such different resistivity response to SDW ordering is helpful to understand what role the SDW ordering plays in Fe-based high- T_c superconductors. Inset shows the anisotropy of resistivity (ρ_c/ρ_{ab}). The resistivity anisotropy, ρ_c/ρ_{ab} , is about 50. Anisotropy in CaFe_2As_2 is less than 150 of BaFe_2As_2 . This could arise from that the interaction between the Ca layer and FeAs layer is much stronger than that between the Ba layer and FeAs layer. Such strong coupling along c -axis leads to an apparent contraction of about 0.13 nm in c -axis lattice, the c -axis lattice parameter decrease from 1.302 nm in BaFe_2As_2 to 1.173 nm in CaFe_2As_2 . A almost temperature independent ρ_c/ρ_{ab} suggests that in-plane and out-of-plane transports share the same scattering mechanism.

Temperature dependences of Hall coefficient and thermoelectric power (TEP) for single crystal CaFe_2As_2 are shown in Fig. 4. TEP of CaFe_2As_2 is negative in high temperature range, and changes the sign at about 165 K and shows a complicated temperature dependence. TEP slightly increases with decreasing temperature to about 170 K, and then a big jump increase is observed due to the SDW transition or structural transition. Below 145 K, TEP slowly increases with decreasing temperature to about 110 K, then decreases monotonously. A similar big jump around 140 K was observed in BaFe_2As_2 , but a negative sign is opposite to that of CaFe_2As_2 [7]. The Hall coefficient of CaFe_2As_2 is negative and changes to positive above 260 K. The temperature dependence of Hall coefficient is almost independent on temperature between 260 K and 160 K. Below $T_s = 160$ K, a pronounced decrease in Hall coefficient is observed, which coincides with T_s of the SDW transition or structural transition observed in susceptibility and resistivity. The magnitude of Hall coefficient of CaFe_2As_2 at 5 K is about two-order

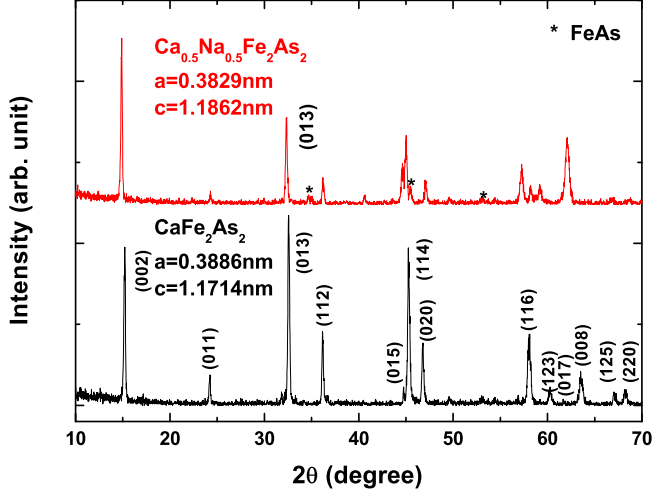


FIG. 5: X-ray powder diffraction patterns at room temperature for the polycrystalline samples: CaFe_2As_2 and $\text{Ca}_{0.5}\text{Na}_{0.5}\text{Fe}_2\text{As}_2$, respectively.

smaller than that of parent compound of LaOFeAs with single FeAs layer [17]. It indicates a higher carrier density in two-layers compounds. The opposite sign of Hall and thermoelectric power is different with parent compound LaOFeAs [17], in which sign of Hall coefficient and thermoelectric power are both negative. Similar results are also reported in EuFe_2As_2 compound [18]. These results indicate a multiband scenario in parent compounds with two FeAs layers in a unit cell.

X-ray powder diffraction patterns are shown in Fig. 5 for the polycrystalline samples: CaFe_2As_2 and $\text{Ca}_{0.5}\text{Na}_{0.5}\text{Fe}_2\text{As}_2$. Nearly all diffraction peaks in the patterns of CaFe_2As_2 and $\text{Ca}_{0.5}\text{Na}_{0.5}\text{Fe}_2\text{As}_2$ can be indexed by the tetragonal ThCr_2Si_2 -type structure, indicating that the samples are almost single phase. The lattice parameters are $a=0.3886\text{ nm}$ and $c=1.1714\text{ nm}$ for the sample CaFe_2As_2 and $a=0.3829\text{ nm}$ and $c=1.1862\text{ nm}$ for the sample $\text{Ca}_{0.5}\text{Na}_{0.5}\text{Fe}_2\text{As}_2$, respectively. It indicates that Na doping leads to an apparent decrease in a -axis lattice and an increase in c -axis lattice. This result is similar to $\text{Ba}_{1-x}\text{K}_x\text{Fe}_2\text{As}_2$ [5].

Figure 6 shows temperature dependence of resistivity for polycrystalline samples: CaFe_2As_2 and $\text{Ca}_{0.5}\text{Na}_{0.5}\text{Fe}_2\text{As}_2$. Polycrystalline parent compound shows similar behavior to that of corresponding single crystal. Similar temperature-linear dependent resistivity is observed above the anomaly temperature. The anomaly for increase in resistivity for polycrystalline sample is much weak relative to that observed in single crystal. Compared to the single crystal, the transition temperature in polycrystalline sample is about 10 K higher. As shown in Fig. 6, no anomaly in resistivity is observed and a superconducting transition at 20 K shows

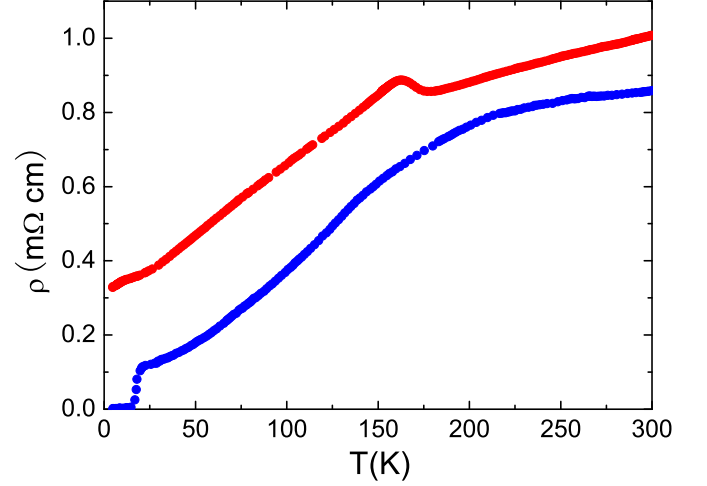


FIG. 6: Temperature dependence of resistivity for polycrystalline samples: CaFe_2As_2 and $\text{Ca}_{0.5}\text{Na}_{0.5}\text{Fe}_2\text{As}_2$, respectively. The anomaly is completely suppressed and a superconductivity at about 20 K is observed.

up in sodium doped sample $\text{Ca}_{0.5}\text{Na}_{0.5}\text{Fe}_2\text{As}_2$. It suggests that partial substitution of Na for Ca induces hole-type carrier into system, and leads to the suppression of structural and SDW instabilities and induces superconductivity in $\text{Ca}_{0.5}\text{Na}_{0.5}\text{Fe}_2\text{As}_2$. Such behavior is consistent with that reported in electron-doped $\text{RFeAsO}_{1-x}\text{F}_x$ (R =rare earth) system [1, 9, 10, 18] and hole-doped $\text{M}_{1-x}\text{K}_x\text{Fe}_2\text{As}_2$ (M =Ba and Sr) system [5, 7, 11, 12].

In summary, we systematically study the anisotropy of resistivity and susceptibility in high-quality single crystal of parent compound CaFe_2As_2 . The resistivity anisotropy ($\rho_{c=ab}$) is about 50, and small relative to BaFe_2As_2 due to stronger coupling between the Ca layer and FeAs layer than that between the Ba layer and FeAs layer. An apparent contraction along c -axis of about 0.13 nm is observed. Temperature independent resistivity indicates that the transport in ab plane and along c -axis direction shares the same scattering mechanism. The susceptibility behavior is very similar to that of antiferromagnetic SDW pure chromium and BaFe_2As_2 . In sharp contrast to the case of other parent compounds ROFeAs (R =rare earth) and MFe_2As_2 (M =Ba and Sr), SDW ordering (or structural transition) leads to a steep increase of resistivity. Such different resistivity response to SDW ordering is helpful to understand the role played by SDW ordering in Fe-based high- T_c superconductors. Partial substitution of Na for Ca induces hole-type carrier into system, leading to the suppression of structural and SDW instabilities and induces superconductivity at 20 K in $\text{Ca}_{0.5}\text{Na}_{0.5}\text{Fe}_2\text{As}_2$.

Acknowledgment: This work is supported by the Nature Science Foundation of China and by the Min-

istry of Science and Technology of China (973 project No: 2006CB601001) and by National Basic Research Program of China (2006CB922005).

Corresponding author; Electronic address:
chenxh@ustc.edu.cn

- [1] Y. Kamihara et al., J. Am. Chem. Soc. 130, 3296 (2008).
- [2] X. H. Chen et al., Nature 453, 761 (2008).
- [3] G. F. Chen et al., Phys. Rev. Lett. (in press) (2008).
- [4] Z. A. Ren et al., arXiv:0803.4283v1 (2008).
- [5] M. Rotter, M. Tegel and D. Johrendt, arXiv:0805.4630v1 (2008).

- [6] C. Cruz et al., arXiv:0804.0795 (2008).
- [7] G. Wu et al., arXiv:0806.2452 (2008).
- [8] Q. Huang et al., arXiv:0806.2776 (2008).
- [9] R. H. Liu et al., arXiv:0804.2105 (2008).
- [10] J. Dong et al., arXiv:0803.3426 (2008).
- [11] G. F. Chen et al., arXiv:0806.1209 (2008).
- [12] K. Sasmal et al., arXiv:0806.1301 (2008).
- [13] M. Rotter et al., arXiv:0805.4021 (2008).
- [14] M. P. Sterer and G. Nagorsen, Z. Naturforsch. B: Chem. Sci. 35, 703 (1980).
- [15] G. M. Sheldrick, SHELX-97, Program for X-ray Crystal Structure Solution and Refinement. Göttingen University Germany (1997).
- [16] E. Fawcett et al., Rev. Mod. Phys. 61, 25 (1994).
- [17] M. A. McGuire et al., arXiv:0804.0796 (2008).
- [18] Z. Ren et al., arXiv:0806.2591 (2008).